Influence of DC electric field upon the production of oil-in-water-in-oil double emulsions in upwards mm-scale channels at low electric field strength

Alberini, Federico; Dapelo, Davide; Enjalbert, Romain; Van Crombrugge, Yann; Simmons, Mark J.h.

DOI:
10.1016/j.expthermflusci.2016.10.023

Document Version
Publisher's PDF, also known as Version of record

Citation for published version (Harvard):
Alberini, F, Dapelo, D, Enjalbert, R, Van Crombrugge, Y & Simmons, MJH 2017, 'Influence of DC electric field upon the production of oil-in-water-in-oil double emulsions in upwards mm-scale channels at low electric field strength', *Experimental Thermal and Fluid Science*, vol. 81, pp. 265-276.
https://doi.org/10.1016/j.expthermflusci.2016.10.023

Experimental Thermal and Fluid Science 81 (2017) 265–276

Contents lists available at ScienceDirect

Experimental Thermal and Fluid Science

journal homepage: www.elsevier.com/locate/etfs

Influence of DC electric field upon the production of oil-in-water-in-oil double emulsions in upwards mm-scale channels at low electric field strength

Federico Alberini [a,*], Davide Dapelo [b], Romain Enjalbert [a], Yann Van Crombrugge [a], Mark J.H. Simmons [a]

[a] School of Chemical Engineering, University of Birmingham, B15 2TT, UK
[b] School of Civil Engineering, University of Birmingham, B15 2TT, UK

ARTICLE INFO

Article history:
Received 31 March 2016
Received in revised form 18 October 2016
Accepted 20 October 2016
Available online 21 October 2016

Keywords:
Double emulsion
High speed imaging
Image analysis
Drop diameter
Flow regime
Electric field

ABSTRACT

A novel approach to create O/W/O is developed and described to achieve uniform oil drop size coated with thin layers of water. Drops were created using a test cell where the DC field is applied between different internal diameter (ID) needles (from which the O/W emulsion emits upwards into a continuous oil phase) and a grounded metal ring which was located at selected distances from the needle top. The advantages compared to the previous techniques consist of possibility of control on drop size and coating layer of the water using low electric field. A high speed imaging technique has been applied to determine drop size under different flow and electric field conditions. Without the electric field, several flow regimes were observed; stable formation of both the O/W/O emulsion and the O/W emulsion upstream of the cell was possible over a range of Reynolds numbers from 80 to 100. The effect of the electric field was found to be reverse below electric field strength of 60 kV m^{-1}, beyond this critical value there was significant impact upon the flow regime, drop size and emulsion structure. The impact of the electric field strength upon flow pattern and emulsion structure and a quantitative analysis of droplet size are presented. The work shows the results for the controlled creation of complex emulsion droplets combining electric field and mm scale channels. The differences with the other physical processes reported in the literature are discussed.

1. Introduction

The demand for new complex multiphase liquid products, particularly in the food, pharmaceutical and cosmetic industries, have driven the need for a deep understanding of how emulsions are formed and stabilised [1,2]. A double emulsion is comprised of droplets dispersed in a continuous phase to form a primary emulsion, which is then dispersed within an outer continuous phase forming the secondary emulsion [3]. Industrial applications of double emulsions are diverse, including low fat and low salt food products which maintain the texture and mouth feel of conventional high fat and high salt products [4,5] or controlled drug release mechanisms [6]. Whilst research on single emulsions has been largely developed over the last few decades [7]; recent efforts have focussed on double emulsions so that their potential use in multiphase products can be fully exploited.

Double emulsions can be produced using several different methods. In most cases, multiple emulsions are prepared according to a two-step process [8]; each step comprises the addition of a dispersed phase and its corresponding emulsifying agent (usually a surface active molecule, or particle). Each step may be carried out using processes including, for example, hollow fibre membranes or homogenisers [9]. However, these methods can be difficult to control and possible destabilization pathways include rupturing of the primary emulsion droplets in the second re-emulsification step [10]. This destabilization pathway may be avoided if one-step processes such as micro-fluidics are used [8], which exploit tightly controlled laminar flow conditions [11,12]. Despite their obvious potential, scale-up and fouling (blocking) of the micro channels remain obstacles.

An alternative method is the electro spraying technique which has been investigated extensively over the two centuries [13–19]. Bose and Nollet were the first to investigate the effect of an applied electric field on the formation of liquid droplets from a jet, illustrating a reduction of drop size as a function of the applied field strength. This has been noted in many works since [20–22].

* Corresponding author.
E-mail address: f.alberini@bham.ac.uk (F. Alberini).

http://dx.doi.org/10.1016/j.expthermflusci.2016.10.023
0894-1777/

Normally, electro spraying involves high values of electric field strength usually above 10^6 V m^{-1} [24,25] and the key phenomenon is the induced charge at the interface between an electrically conducting liquid and the continuous phase. Beyond a certain critical level, the interface becomes unstable and evolves from a generally rounded shape to another including one or several remarkably stable conical features called Taylor cones [17].

Another phenomenon, which can occur when an electric field is applied, is the electro-hydrodynamic flow [23,26,27]. When a neutral leaky dielectric drop is immersed in a continuous conductive phase, flow motion is generated by action of the applied electric field on the continuous phase. Taylor [28] introduced the leaky dielectric model to describe the electro-hydrodynamic deformation of a drop. The theory applies to weak electric fields, where drop deformation is small [29].

In the last few decades, numerical solutions of the governing equations have been made possible using computational methods and these have been used primarily to quantify the dynamics of droplets exposed to electric fields but mostly in single emulsions [23,30,31].

Most recently, analytical work and modelling techniques (finite element) have been used to explore how the dynamics of the creation of double emulsions may be altered by the presence of an electric field [32,33]. Some limited work has been carried out on how double emulsion drops may be made highly concentric by use of an applied AC field [34]. However, in the open literature there still remains a dearth of validated computational and experimental studies on the formation of double emulsions which combine both electric fields and micro or macro channels.

The work presented in this paper is concerned with the experimental investigation of the continuous formation of oil-in-water-in-oil (O/W/O) double emulsions under the effect of a DC electric field. The upwards needle set up allows the formation of stable primary emulsion which was not possible to achieve using the most extensively used downwards set up. The effects of flow rate and low electric field strength ($\sim 10^5$ V m^{-1}) upon the flow patterns and types of double emulsion drops are observed and used to catalogue the different flow regimes with reference to the stability and repeatability of double emulsion formation. The observed results have been used to describe the existence of this phenomenon which differentiates from the better known electrospraying, electro-dripping and electro-hydrodynamic flows. The production of double emulsion using low electric field presents advantages compared with others techniques previously described in the literature. A tighter control of secondary emulsion drop size towards smaller or larger scale can be achieved applying a low electric field. In fact, before a critical value of the electric field is achieved, the water drops tend to increase in size. After the critical value the drops decreases towards a minimum where a thin water coating layer is formed on top of oil drops. If compared with the hollow fibre membrane and homogenisers, this technique has lower potential costs of manufacture and better process control. Finally, compared to micro-fluidic devices, this technique is a valid alternative for the production of double emulsions and it is not much affected by the fouling issues.

2. Materials and methods

2.1. Fluids and fluid properties

The specification and suppliers of all fluids and chemicals used in the experiments are given in Table 1, together with their bulk properties. For all the experiments, Lytol, a low viscosity transparent mineral oil, was used as the organic phase and distilled water was used as the aqueous phase. The relative permittivity and absolute permittivity of the oil are presented in Table 1. The conductivities of the fluids were measured using a RS CD-4303 conductivity meter to an accuracy of ±0.01 μS cm^{-1}. The values obtained for the Lytol oil, pure distilled water and distilled water with SLES at a concentration of 1.4 times the critical micelle concentration (CMC) are reported in Table 1.

Table 1
Relevant physical properties of the materials used in the system.

Material	Lytol	Distilled water	Water + SLES
Density at 20 °C (kg m^{-3})	800	1000	1000
Dynamic viscosity (Pa s)	0.0051	0.001	0.001
Relative permittivity	2.1	~80	N/A
Absolute permittivity ε (F m^{-1})	$1.89 \cdot 10^{-11}$	N/A	N/A
Conductivity (μS cm^{-1})	0 ± 0.01	0.5 ± 0.01	21.64 ± 0.01

Chemicals	Product specification	Supplier
Lytol oil	Lytol oil	Lytol
Distilled water	Distilled water	University of Birmingham
SLES	Texapon N701	BASF
Nigrosin	Alcohol soluble	Sigma-Aldrich
Span 80	Span 80	Sigma-Aldrich

The organic soluble and aqueous soluble surfactants used were commercial grades of sorbitane monooleate (Span 80) and sodium lauryl ether sulphate (SLES) respectively. Alcohol soluble Nigrosin was used as black dye in the inner oil phase to distinguish clearly between the two different dispersed phases in the images.

The surface and interfacial tensions of the fluids were measured using the Wilhelmy plate method using (Kruss K100 tensiometer) as shown in Table 2. These were first measured as pure fluids and then as fluids with the appropriate concentrations of surfactant used in the experiments. The critical concentration of Span 80 in the oil phase to enable stable formation of the primary O/W emulsion was found to be 0.5 wt%. The CMC of SLES was calculated and a value of 0.2 mol m^{-3} was obtained which corresponds to the literature value [35]. For the experiments, 1.4 times the critical micelle concentration (CMC) of SLES was used to reach a stable primary emulsion. In order to verify the influence of Nigrosin dye on the interfacial tension of the oil phase, measurements with and without the dye were performed. No difference was observed.

2.2. Experimental rig

A schematic of the experimental rig is given in Fig. 1a. The specifications of the equipment used are given in Table 3, including the dimensions of the needle electrode. The electric field was generated using a Glassman DC power supply. The applied voltage ranged from 2 kV to 20 kV in steps of 2 kV. The DC cable from the supply was attached to the needle electrode at the bottom of the rig and the ring electrode at the top of the continuous oil chamber was grounded. The entire rig was inserted into a protective Perspex chamber which was interlocked to the power supply to prevent accidental exposure of the operator to the electric field.

With reference to Fig. 1a, the oil phase (dyed with Nigrosin) was pumped into the system using a syringe pump (I) and a gastight glass syringe. The water phase was injected using a syringe pump (L) equipped with a Monoject 140 mL plastic syringe. Due to the buoyancy forces caused by the density differences between the oil and water, the rig was oriented so that the fluids flow vertically upwards. This is a known limitation for wide channels and it can limit the repeatability of the process if the needle is oriented vertically downwards or horizontally.

The single O/W emulsion was produced within a T-piece (A) (ID = 3×10^{-3} m) schematised in Fig. 1b. Oil and water were injected separately through 0.37 mm ID needles through each

Table 2
Measured surface and interfacial tensions of relevant fluids.

Surface tensions · 10^{-3} (N m^{-1})			Interfacial tensions · 10^{-3} (N m^{-1})	
Oil	Oil with 0.5 wt% Span 80	Water with 0.012 wt% SLES	Water with 0.012 wt% SLES-Oil	Water with 0.012 wt% SLES-Oil with 0.5 wt% Span 80
28.53	28.40	31.39	13.15	0.97

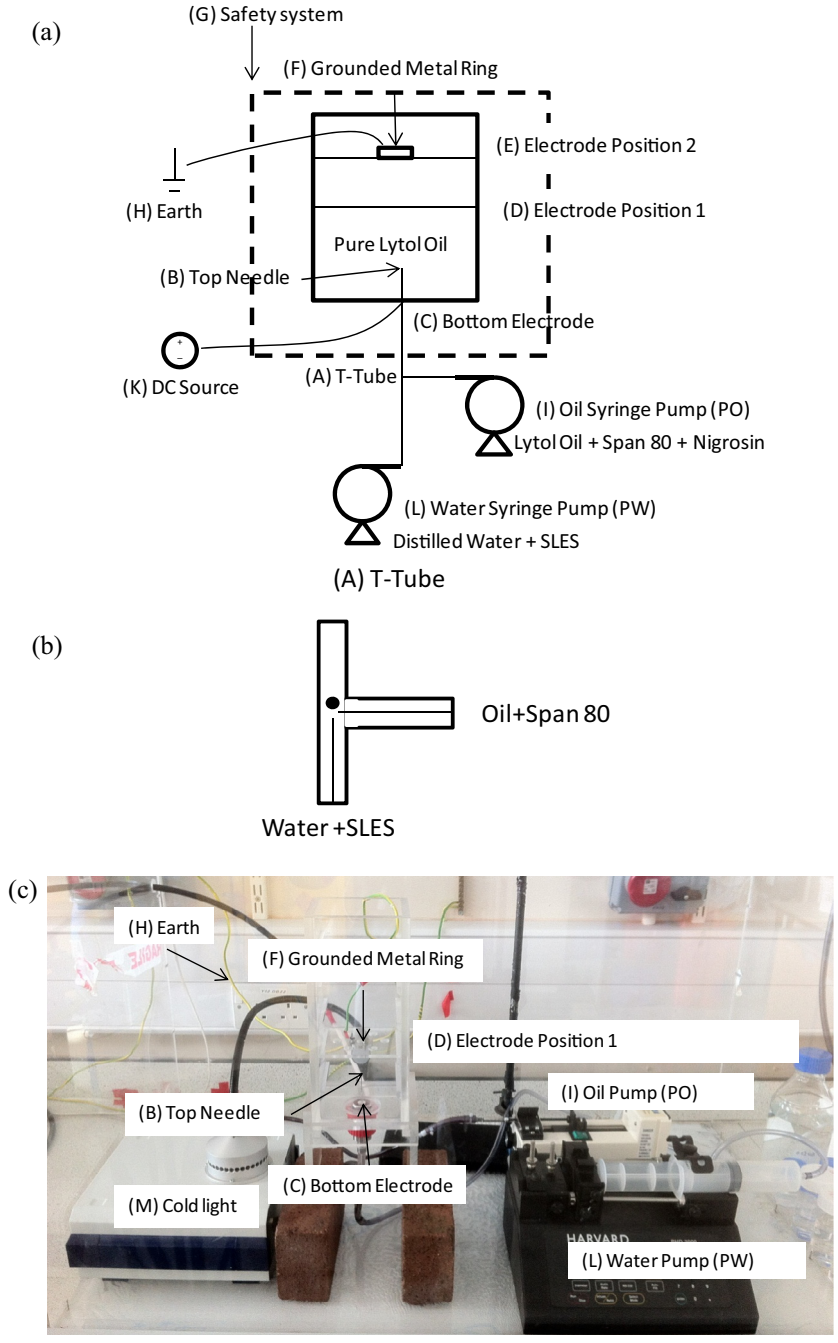

Fig. 1. The experimental set-up: (a) Schematic rig, (b) T-Tube, (c) picture of the rig.

arm of the T-piece respectively. The single O/W emulsion then flowed up through the top needle (B) (Fig. 1a) using either 0.8 or 1.6 mm ID needles into a continuous oil phase producing the O/W/O double emulsion. The location of the grounded metal ring (F) was fixed either at position 1 (D) or position 2 (E) which are 130 and 170 mm above the bottom electrode (C) respectively. A quantity, called electric field strength and with the same dimensions of an electric field (V m^{-1}) can thus be calculated for position 1 or position 2 by dividing the supplied voltage by the distance between the bottom electrode (C) and the grounded metal ring (F) within a range between 0 up to 160 kV m^{-1}.

Experiments were performed at fixed values of applied voltage per unit length but using a combination of different voltages and different lengths. Such quantity cannot be formally identified with

Table 3
Dimensions of all needles and the specifications of the equipment used.

Needle gauge	22	18	14
Inner diameter, $\cdot 10^{-3}$ (m)	0.37	0.8	1.6
Outer diameter, $\cdot 10^{-3}$ (m)	0.72	1.27	2.1

Apparatus	Model	Supplier
Tensiometer	K100	Krüss
Water still	A4000D	Aquatron
Needle gauge	14 (B), 18 (B), 22 (A).	SGE Analytical Science
Oil pump (PO) (I)	A-99	Razel Scientific Instruments
Water pump (PW) (L)	PHD2000	Harvard Apparatus
Glass syringe (I)	Gastight 1001	Hamilton
Monoject syringe (L)	140 mL	Covidien
DC electric field (H)	High Voltage EQ Series DC	Glassman
Safety system (G)	Guardmaster Centurion	Allen-Bradley
Cold light (M)	KL5125	Krüss

an electric field as the electric field is not a constant quantity within our experiment setup. This was done to confirm if the applied voltage per unit length was indeed the dominant factor as it was for [25], or whether the absolute potential change in field pattern due to a change in geometry was important.

2.3. Flow visualisation

A high speed camera (Fastcam SA3, Photron Ltd, Japan) equipped with a Navitar 12X ZoomXtender lens was used to capture all the images. Frame rates between 250 and 2000 fps were used. These were selected as appropriate to capture best the dynamics of the system. 10 double emulsion drops were analysed for each case. All data was recorded using the Photron Fastcam Viewer (PFV) software and all image processing of the drops was carried out using ImageJ freeware software. Each drop was assumed to be a oblate ellipsoid, defined by two major dimensions (r_1) and a minor dimension (r_2). Its volume, V_D is thus calculated as:

$$V_D = \frac{4}{3}\pi r_1^2 r_2. \tag{1}$$

To verify this assumption a simple mass balance has been used combining the information obtained from images and the values of flow rates used for the experiments. The calculated flow rate values agree with experimental values within a range 10%.

The equivalent sphere diameter, d_{ESD} can then be calculated using

$$d_{ESD} = \sqrt[3]{\frac{6\,V_D}{\pi}}. \tag{2}$$

For the higher frame rates, a cold light source was used as background lighting. The use of a cold light source avoided any rise in temperature of the fluids which would affect their surface and bulk properties.

2.4. Flow conditions

Table 4 illustrates the five water flow rates used for each needle size, showing the initial ranges used for the determination of the stable regions for emulsion creation. The flow rates used within the stable region were chosen so that experiments could be done with both 0.8 ID and 1.6 mm ID needles at the same values of Reynolds numbers. The Lytol flow rate was fixed at 8.125×10^{-10} m^3 s^{-1} for all the conditions used. For the calculation of Reynolds numbers only the flow rate of water has been considered because the flow rate of oil is negligible (three orders of magnitude smaller than the water flow rate).

3. Theory

A dimensional analysis of the problem leads to the identification of several key dimensionless groups. The capillary number represents the ratio of viscous to interfacial forces between two separate immiscible phases expressed as follows:

$$Ca = \frac{\mu_c u}{\gamma} \tag{3}$$

where μ_c is the dynamic viscosity of the continuous phase (Pa s), u is a characteristic velocity (m s^{-1}) and γ is the interfacial tension (N m^{-1}). Under the action of an applied electric field, an equivalent electrical capillary number, interchangeably called the electrical Weber or Bond number, may be defined as:

$$Ca_e = \frac{d_{ESD} AV_{PUL}^2 \varepsilon}{\gamma} \tag{4}$$

This electrical capillary number quantifies the ratio of the electrical stress to the interfacial tension. AV_{PUL} symbolizes the applied voltage per unit length (V m^{-1}) which is defined by:

$$AV_{PUL} = \frac{V}{l}, \tag{5}$$

where V is the voltage (V) and l is the distance between the two electrodes (m). This quantity has the dimension of an electric field strength which does not correspond to the absolute value of electric field acting on the drop. However, this value can be used as a constant to compare experiments at different AV_{PUL}. Moreover, its bulk effect on the drops does not change if the ratio of V over l (varying the applied voltage and the distance between the electrodes to obtain similar ratios) is maintained constant. Later in the results this aspect will be demonstrated in details. The other parameter is ε (F m^{-1}) which is the permittivity of the continuous phase of the secondary emulsion (see Table 1).

The Reynolds number of flow has also been evaluated as:

$$Re = \frac{\rho_c u d}{\mu_c} \tag{6}$$

where ρ_c represents the density of the continuous phase (kg m^{-3}), d is the diameter of the needle or drop (d_{ESD}) (m) and u is the velocity of the water flow or of the water drop. As will be shown later, the droplet may have a diameter which is substantially larger or smaller than the diameter of the needle, this is compensated for in the

Table 4
Flow rates used at the different needle gauges and their corresponding Reynolds numbers in the channel and Reynolds numbers of drop.

Needle ID (mm)	0.8					1.6				
Flow rate $\cdot 10^{-7}$ (m^3 s^{-1})	0.12	0.50	0.58	1.85	3.70	0.24	1.00	1.17	3.70	7.4
Reynolds Number	20	80	93	300	600	20	80	93	300	600
Refer to Fig. 2	A	B	B	C	D	A	B	B	C	D
Reynolds Number drop at 0 kV m^{-1}	/	5.20	5.66	/	/	/	9.56	11.79	/	/

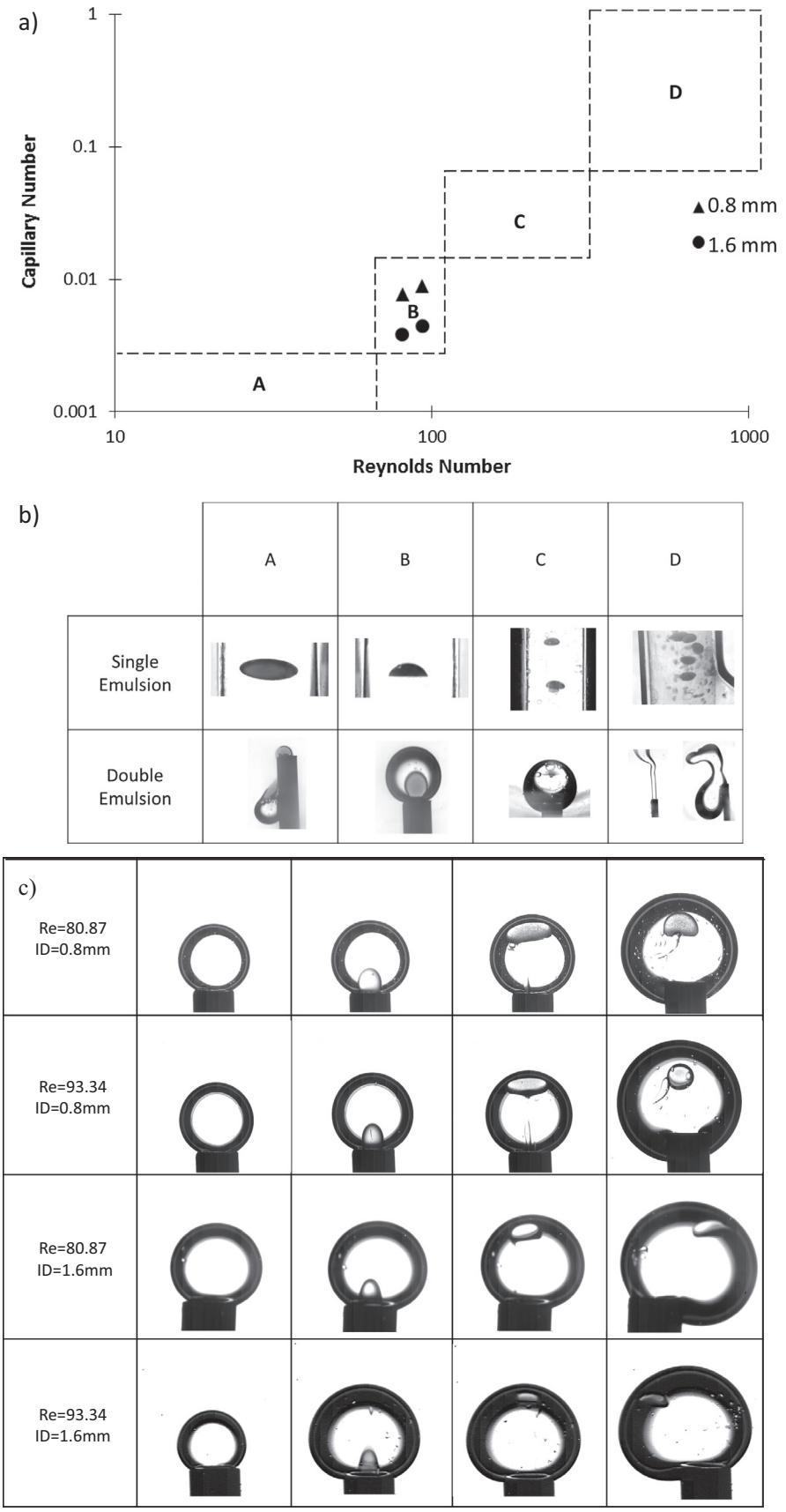

Fig. 2. Flow regimes in the system at various needles ID and flow rates: (a) Plot of Reynolds number versus capillary number, (b) single and double emulsion at different flow regimes and (c) double emulsion for regime B at different Reynolds numbers.

calculation of the initial drop velocity upon detachment from the needle using a conservation of volume argument i.e.

$$u_D = \frac{3}{2} u \frac{d^2}{d_{ESD}^2} \quad (7)$$

where u is the superficial velocity of the water flow in the needle, d is the needle diameter and d_{ESD} is the spherical equivalent diameter of the drops at detachment. Eq. (7) has been derived from a simple mass balance based on drop volume per unit time equal to flow rate. Δt is the time in which a drop is formed and it can be estimated as the ratio of d_{ESD} divided by u_D or the volume of the drop divided by the cross section of the pipe multiplied the superficial velocity. Equalising these two estimations of Δt the Eq. (7) can be derived. Using (6) and (7), the values of Reynolds number for the drop (Re_D) are shown in Table 4.

4. Results and discussion

4.1. Formation of double emulsion without electric field

Experiments have been carried out over a range of capillary and Reynolds numbers to identify possible regions where stable single and double emulsions could be produced as shown in Fig. 2a, without the electric field (Table 4). Fig. 2b shows pictures of the single and double emulsion drops formed at the needle electrode for each of the regions A-D identified in Fig. 2a.

In region A ($Re < 80$), the single emulsion suffered in that the oil drop occupied almost all of the O/W emulsion volume, thus a secondary emulsion could not be formed. In region B ($80 < Re < 100$), single and double emulsions were consistently produced. At higher Reynolds number in region C, the inner oil droplets produced in the single emulsion become unstable and jetting was eventually observed (region D). The oil drops created in the "T" junction had a consistent oil drop size when re-measured at the outlet of the top needle. In the stable regime (B) the ratio between the oil drop size measured in the single emulsion (i.e. in "T" junction) and the oil drop in the double emulsion (see Fig. 2b) ranged between 1 and 1.5.

These experiments enabled the establishment of a stable regime (B), the most useful for producing good quality multiple emulsions, within which the selection of four operating conditions (2 per needle gauge) were chosen for further study (see Fig. 2a). In Fig. 2c, a sequence of four images for each flow condition is shown. The first column of images on Fig. 2c represents the initial formation of the water drop in the oil continuous phase. After this step the internal oil drop passes inside the water drop. Then the O/W drop detaches from the top needle and the internal oil drop is observed to contact the outer oil-water interface but not merge with it. The last column of images show the maximum size that the water drop achieves, before the detachment of double emulsion drop from the top needle. The needle upward set up, it makes the drop mechanism been different from the mostly used dripping mechanism. In fact, in dripping mode the gravitational force acts simultaneously with the tension surface force from the first instant of drop formation, till its detachment. When the needle is upward, for most of the drop formation time, the gravitational force is balanced by the needle instead. The drop, which is in an unstable gravitational equilibrium on the top of the needle, detaches when the drop is too big to be suspended, and it falls sideways under its own weight.

The formation of the double emulsion is found to be highly repeatable under these conditions. The use of a constant flow rate for the oil allows for the creation of monodisperse oil drops in the

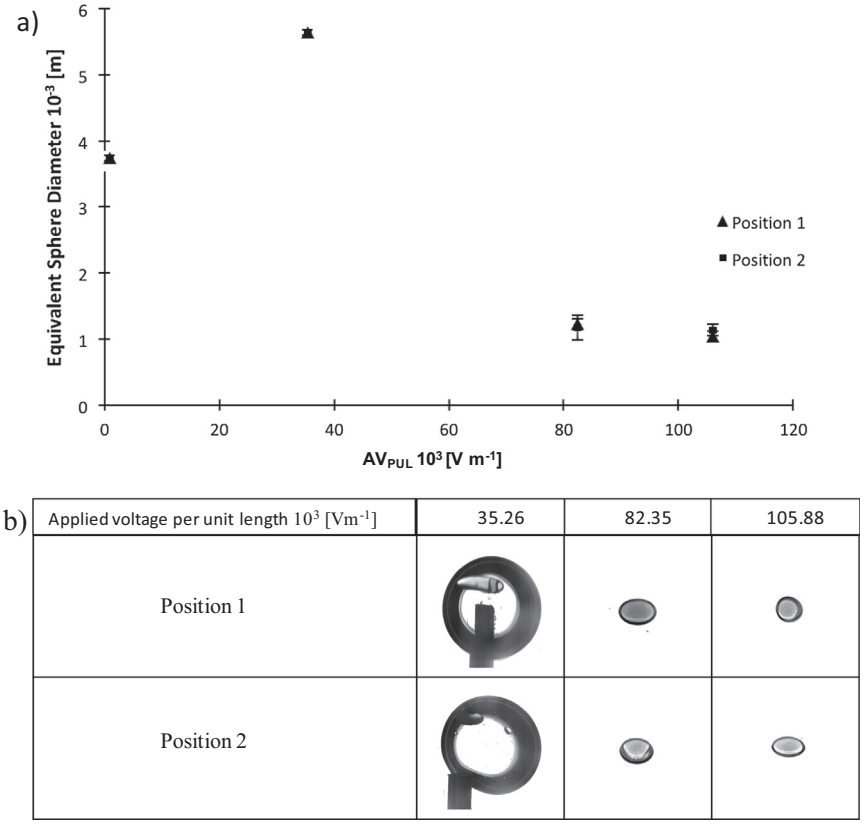

Fig. 3. Effect of electric field per unit length on the water drop sizes for the two different position of earth electrode. The experiments have been investigated at $Re = 93.34$ for the needle with 0.8 mm ID. (a) Equivalent sphere diameter of O/W drop versus electric field strength, (b) images of the drops at different values of electric field per unit length for the two positions.

primary emulsion and a controlled size ratio between the inner oil drop and the water drop which is also directly related to the needles used.

4.2. Formation of double emulsion with electric field

To examine the impact of the electric field on the creation of the double emulsion, three initial experiments were carried out using a constant needle size (ID = 0.8 mm) and Reynolds number (Re = 93.34) with electric field strengths of 35.26, 82.35 and 105.88 kV m^{-1}. Both positions of the top electrode, 1 and 2 as shown in Fig. 1a, were used to ascertain whether electric field strength alone is the critical parameter or whether applied voltage and electrode separation need to be considered. Fig. 3a shows the values of the equivalent sphere diameter obtained at each electric field strength. These values have been found to be independent from electrode position which is confirmed in the work of [24,25] thus applied voltage per unit length (AV_{PUL}) is the key parameter.

Fig. 3b shows images of the corresponding double emulsion drops formed from the needle. All drop measurements have been done just before the drops detach from the needle. The lowest AV_{PUL} has little effect and the large O/W drop begins to fall sideways as it is formed at the needle. For the two highest AV_{PUL} of 82.35 and 105.88 kV m^{-1} the drop is much smaller and contains a much higher fraction of oil. The results show that the dimensions of the drops are comparable for the two positions even if the shape slightly changes in particular at high field strengths.

To understand better the effect of electric field in the system, a more detailed investigation is presented. Fig. 4a shows similar results for the complete study carried out for all four flow conditions (Regime (B)) shown in Fig. 2a. Five values of applied voltage per unit length have been investigated and the values of d_{ESD} for the O/W drop are plotted versus the AV_{PUL} (Fig. 4a).

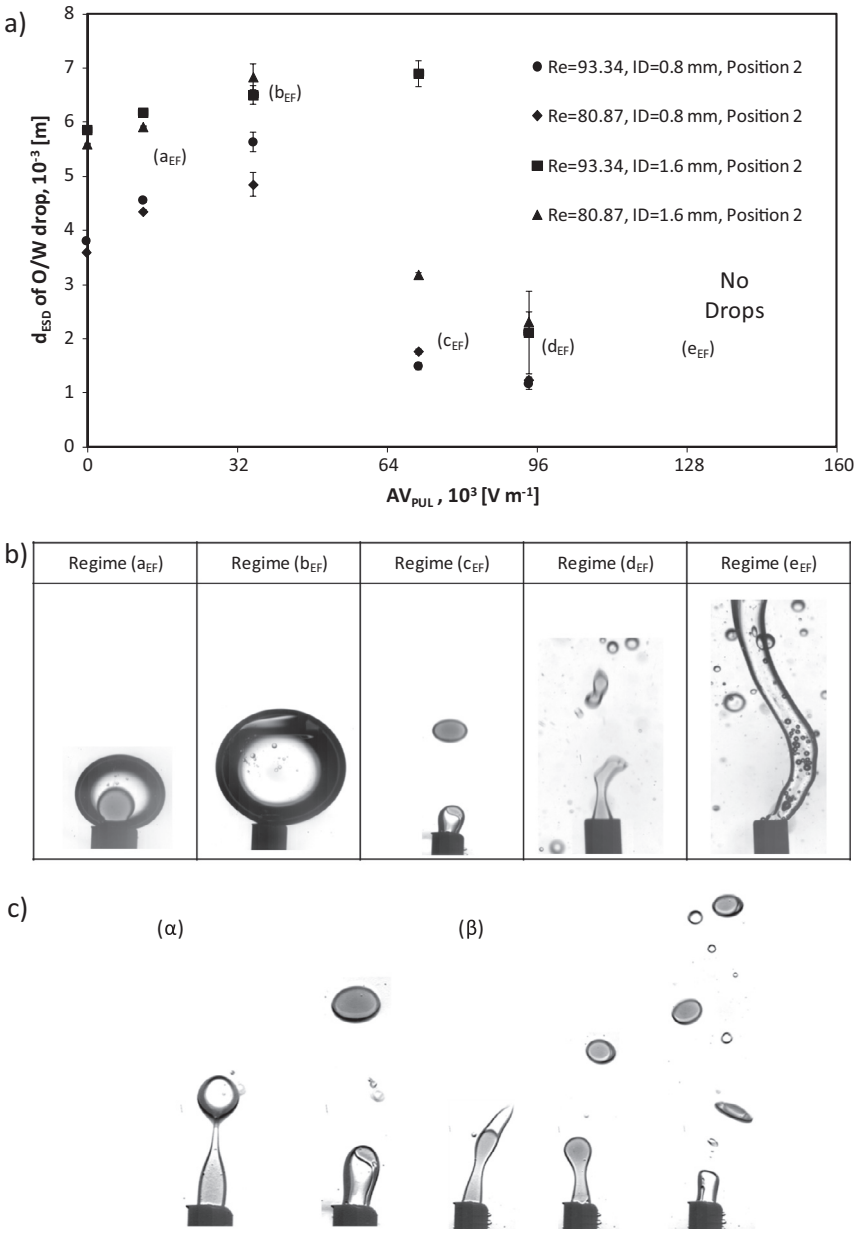

Fig. 4. Flow regimes encountered at the different electric field strength applied to the system for different flow condition and different needle size at constant position. (a) Equivalent sphere diameter versus electric field strength. (b) The images represent the different regimes at the outlet of the top needle. (c) Two different kinds of double emulsion formation for the electric field flow regime (c_{EF}) (α) synchronised formation, (β) unsynchronised formation.

Different electric field flow regimes (a_{EF}:e_{EF}) can be identified as a function of the AV_{PUL} (see Fig. 4b). Regime (a_{EF}) occurs when the effect of the field is negligible and the volume of the water droplet is entirely dependent on the needle size and the flow rate of water. In regime (b_{EF}) the effect of the applied electric field is characterized by a large increase in the O/W drop size. This phenomenon entails an accumulation of more water into the drop which explains the larger drop than at similar fluid flow conditions with 0 kV. However, when a critical value of AV_{PUL} is exceeded the water drops start to decrease in size. The system then enters regime (c_{EF}), which corresponds to a reduction of drop size. In this regime (c_{EF}) above the critical AV_{PUL}, the force of the field detaches the drops of water rapidly as they are formed. This causes a significant decrease in the O/W drop sizes. The nature of the double emulsions formed within this regime depends upon how the oil and water drop detachments are synchronised at the needle outlet. If the inner oil droplet has not completely entered the water drop before it detaches the inner oil drop can be split between different O/W drops.

The possible outcomes of these scenarios are shown in Fig. 4c. In Fig. 4c (α), the inner oil droplet leaves the nozzle in synchronisation with the detachment of the water droplet leading to the formation of an oil-rich double emulsion droplet. The structure of this double emulsion is very unique because the oil drop is coated with a thin layer of water. In Fig. 4c (β), the detachment is not synchronised, leading to the formation of double emulsion droplets with non-uniform oil concentrations. Clearly from a repeatability point of view, the case shown in Fig. 4c (α) is favoured. However in both

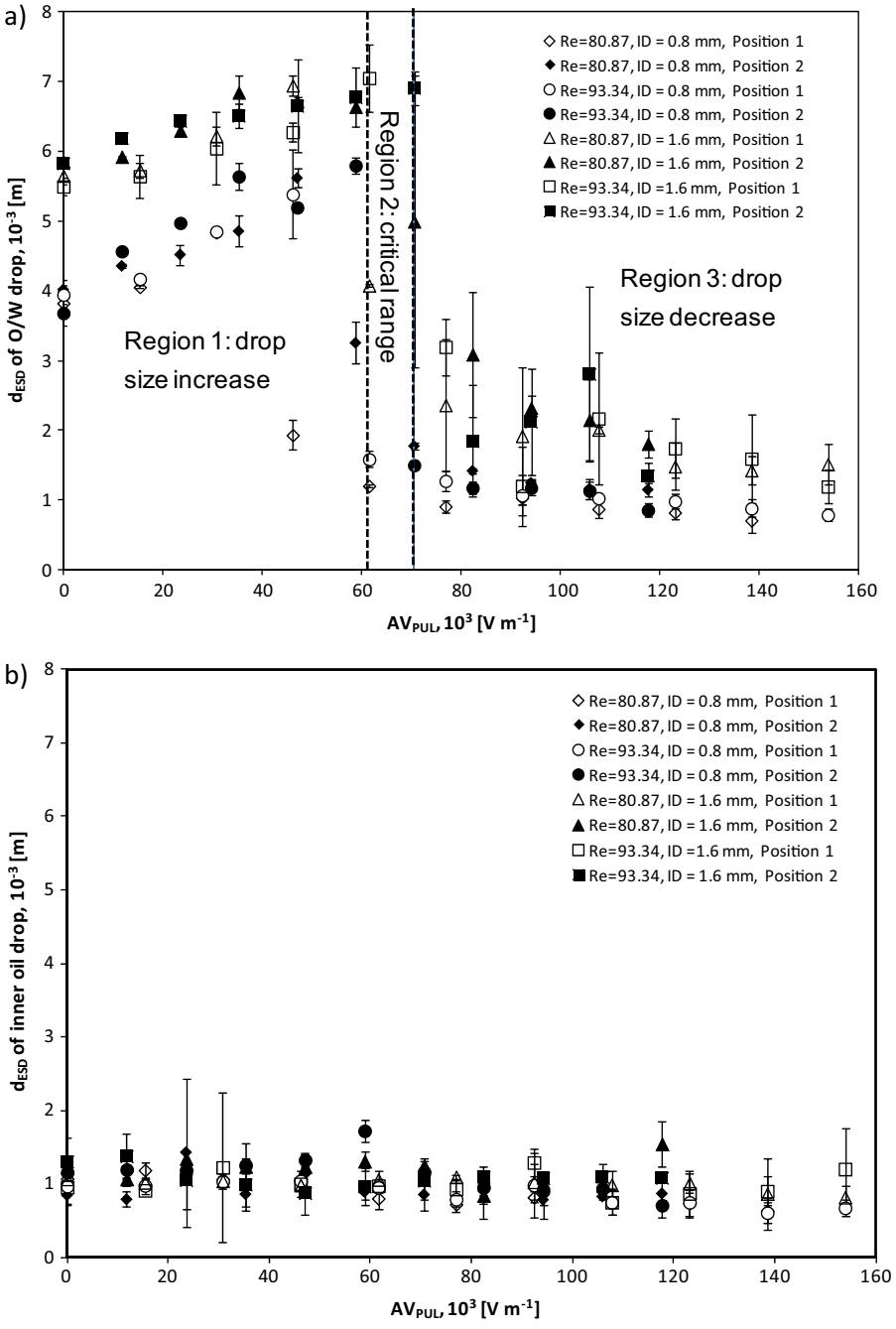

Fig. 5. Equivalent sphere diameter (ESD) of O/W drop (a) and inner oil drop (b) versus electric field per unit length. All set of results are showed for different flow conditions (*Re* = 80.87 and 93.34 in the flow regime (B)), positions and electric field flow regimes (a_{EF}:d_{EF}).

scenarios for this particular regime (c_{EF}), when the drop size is drastically reduced, the diameter distribution is very narrow. This is proved by the almost inexistent error bars in the graph.

Returning to Fig. 4b, Regimes (d_{EF}) and (e_{EF}) correspond to uncontrolled behaviours leading to the formation of unstable and inconsistent structures. In regime (d_{EF}), more drops of water are produced and their movement seems to be more random. The O/W drops are seen to burst releasing the inner oil phase, causing the O/W/O double emulsion to become a W/O single emulsion. For regime (e_{EF}), at the highest voltages (18–20 kV), the high population of small water drops are seen to coalesce spontaneously forming a water filament extending between the electrodes. Due to the formation of this conductive path between the electrodes, this phenomenon activates the rig's safety mechanism, cutting off the power supply.

A summary of the different scenarios are showed in Fig. 5. The obtained d_{ESD} of the O/W drop (Fig. 5a) and the inner oil drop (Fig. 5b) as a function of the AV_{PUL} for all the conditions measured, have been plotted. The data show consistently that the critical AV_{PUL} is between 60 and 70 kV m^{-1} (highlighted by the two dotted lines in Fig. 5a) beyond which the O/W drop size decreases rapidly and then stabilises. Three regions (Fig. 5a) can be identified the first before critical AV_{PUL} range where the drops increase in size, the second where the drops drastically reduce in size (critical range) and the third where the drops decrease in size towards a plateau with the increase of AV_{PUL}.

Conversely, the diameter of the inner oil drops are relatively unaffected by the electric field. Furthermore, Fig. 5b confirms that the constant flow rate of oil produced consistent drop sizes regardless of the varying water flow rates and electric field strengths (within a standard error <10%). The sizes of the oil drops are in the range of 1 up to 1.8 mm and the ratio between the oil drop and the water drop ranges between 5 and 1 with increasing electric field strength.

Finally, to determine the contribution of dynamics effects for the drop break up the dynamic interfacial tension between water

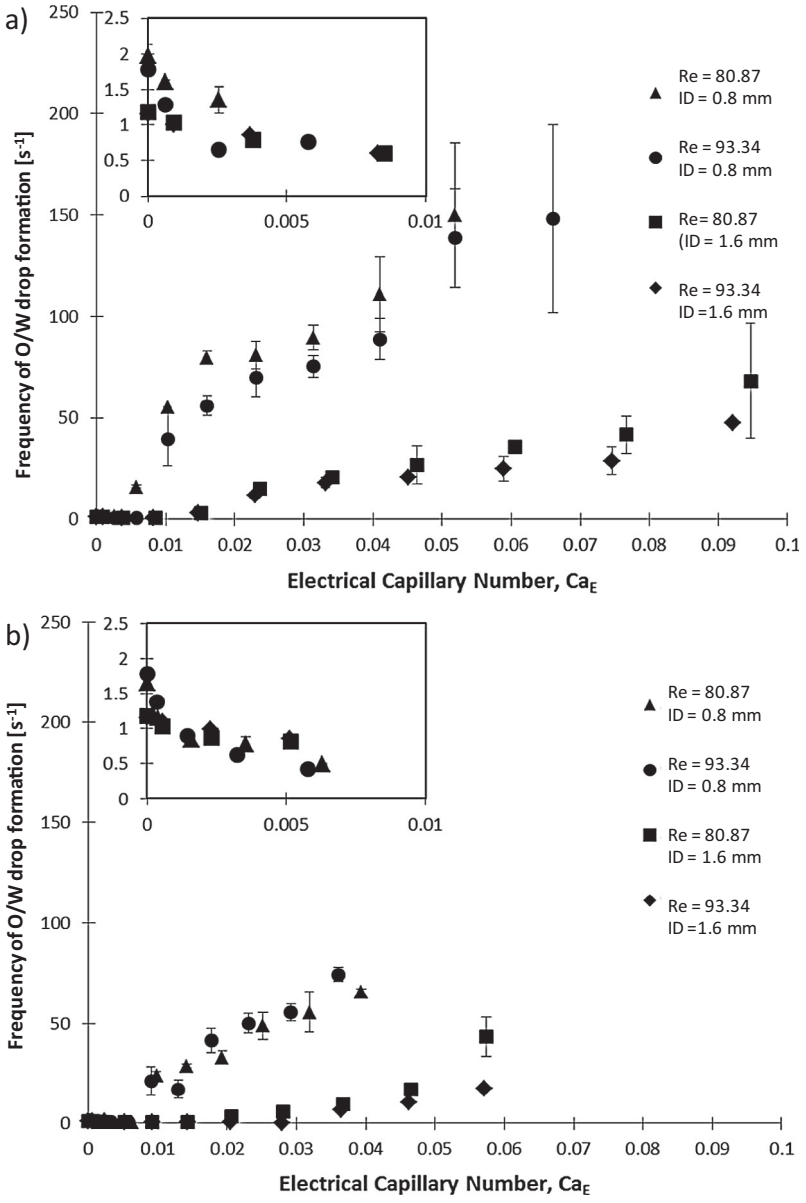

Fig. 6. Frequency of O/W drop formation against electrical capillary number at (a) different flow conditions (*Re* = 80.87 and 93.34 in the flow regime (B)) and electric field flow regimes (a_{EF}:d_{EF}) for the position 1 and (b) at different flow conditions (*Re* = 80.87 and 93.34 in the flow regime (B)) and electric field flow regimes (a_{EF}:d_{EF}) for the position 2.

with 0.5 wt% SLES and air has been measured. The choice of air instead of the oil is due to the difficulty of such measurement. The main assumption is that the surfactant' diffusion coefficient is similar between water/oil and water/air systems. This assumption is justified considering such coefficient as a bulk property. In fact, the diffusion coefficient is reversely proportional to viscosity (in this case of the water and SLES solution) following the Stokes-Einstein equation. This experiment was carried out using the maximum bubble pressure tensiometer (BPA-1S, SINTERFACE Technologies Germany). The obtained results showed that in the time range of 10 ms (5 ms time of formation of drops with electric field and 10 without electric field) the fluid behaves almost as pure liquid. This can be used to prove that the dynamic effects do not play an important role on the drop break up in both cases, with and without electric field.

4.3. Frequency of O/W drop formation

Fig. 6 shows the variation in frequency of the O/W drop formation versus electrical capillary number for different ranges of AV_{PUL}. The different series of data of Fig. 6a and b were achieved applying ranges between 0 and 20 kV, in steps of 2 kV, at position 1 and 2. The values were chosen to enable a wider range of electrical capillary numbers to be explored. The values of frequency have been calculated by counting the number of drops per unit time from sets of images. The results show similar trends in Fig. 6a and b for the two series of data. Before the critical value of AV_{PUL} after which the drop size drastically decreases, it can be seen that the frequency fluctuates around the value of 1 Hz (top left Fig. 6a and b). The needle diameter affects the values of the electrical capillary number after which the frequency of droplet production drastically increases due to the transition to the drop size reduction region as showed in Fig. 5a. This suggests the presence of critical capillary numbers which will be discussed in the following paragraph. To summarise, both needle diameter and flow rate affects the frequency of production with a higher number of droplets being generated with the smaller needle (see Fig. 6a and b).

4.4. Study of the effect of the electric field on O/W drop size

As shown in Fig. 7, the main impact of the electric field is the reduction in size of the O/W drop. In order to determine the influence of interfacial tension forces and effects of convection generated by the electric field, electrical capillary number and Reynolds number are used respectively. Electrical capillary number is used to quantify the deformation of drops and the *Re* number to determine the influence on the fluid flow. In Fig. 7 the ratio of equivalent sphere diameter versus the needle diameter is plotted versus electric capillary number. Above the critical AV_{PUL}, drop size reduction occurred and this value varied for each flow rate, needle and electric field position. Clearly, the aforementioned trend has an initial increase in size in regime (a_{EF}) and then once the system has reached the regime (c_{EF}) the drop sizes tend to decrease. Values of critical electrical capillary number can be estimated from Fig. 7 when the change in regime occurs from increase to reduction of drop size – the values are approximately 0.01 and 0.02 for the 0.8 mm and 1.6 mm needles respectively. Again the results are independent of the distance between the electrodes, as expected.

A plot of Reynolds number, Re_D Eqs. (6) and (7), versus electrical capillary number is shown in Fig. 8. In the steady regime the Reynolds number of the drop slightly decreases due to the drop size

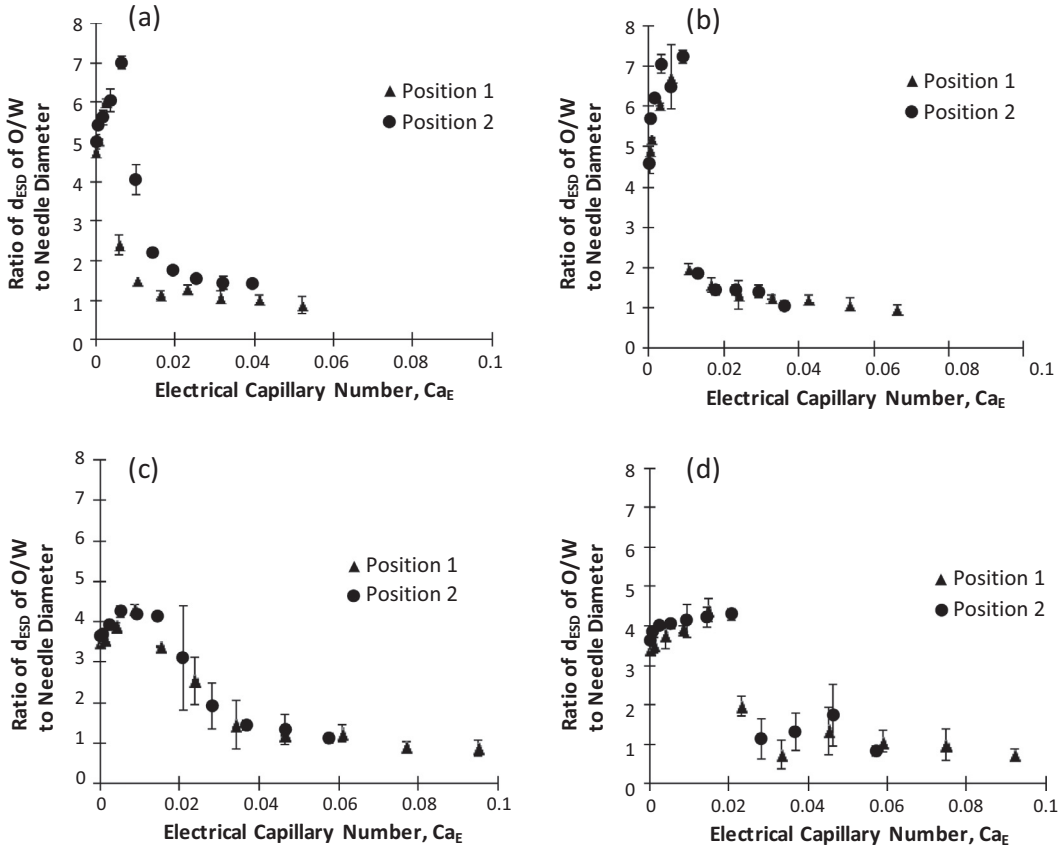

Fig. 7. Plots of equivalent sphere diameter (ESD) of O/W drops against the electrical Capillary number (electric field flow regimes (a_{EF}:d_{EF})) at flow rates of (a) $0.5 \cdot 10^{-7}$ - $m^3 s^{-1}$ (*Re* = 80.87 at 0 kV, 0.8 mm ID), (b) $0.58 \cdot 10^{-7}$ $m^3 s^{-1}$, (*Re* = 93.34 at 0 kV 0.8 mm ID), (c) $1 \cdot 10^{-7}$ $m^3 s^{-1}$ (*Re* = 80.87 at 0 kV, 1.6 mm ID) and (d) $1.16 \cdot 10^{-7}$ $m^3 s^{-1}$ (*Re* = 93.34 at 0 kV, 1.6 mm ID).

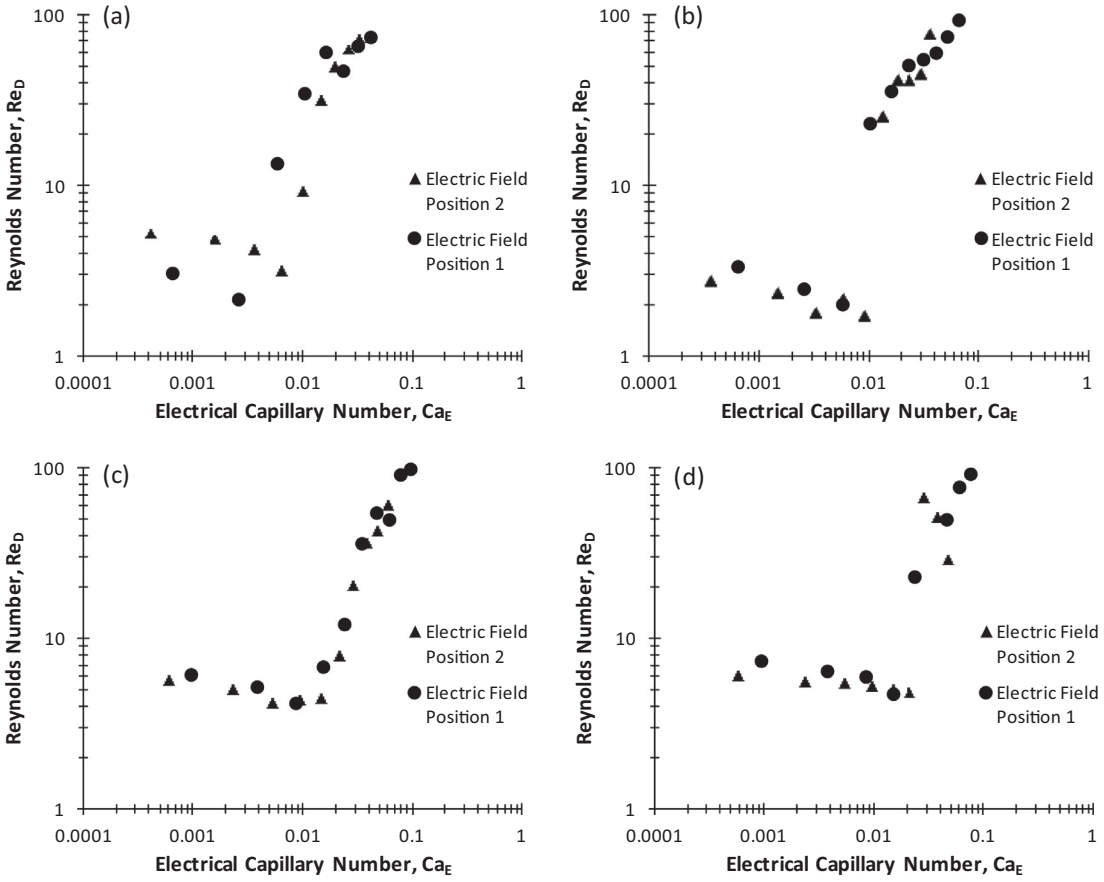

Fig. 8. Log-Log Plots of Reynolds Number against the electrical Capillary number (electric field flow regimes (a_{EF}:d_{EF})) at flow rates of (a) $0.5 \cdot 10^{-7}$ m^3 s^{-1} (*Re* = 80.87 at 0 kV, 0.8 mm ID), (b) $0.58 \cdot 10^{-7}$ m^3 s^{-1}, (*Re* = 93.34 at 0 kV 0.8 mm ID), (c) $1 \cdot 10^{-7}$ m^3 s^{-1} (*Re* = 80.87 at 0 kV, 1.6 mm ID) and (d) $1.16 \cdot 10^{-7}$ m^3 s^{-1} (*Re* = 93.34 at 0 kV, 1.6 mm ID).

increase until the critical value of 60 kV m^{-1}. Increasing the value of AV_{PUL} causes Re_D to increase: the increase of velocity outcompetes the decrease in size of the drops in the numerator of (6). This behaviour is observed in all experiments. The sudden decrease in drop size happens when $Re > 10$. The transition between increase to reduction of drop size happens for $Re_D > 10$. Once in the regime c_{EF}, the increase of AV_{PUL} is proportional to the Reynolds number until it reaches the unstable regime. More difficult is to define a range where the behaviour changes between c_{EF} regime and unstable one.

It can be observed that different Reynolds numbers do not significantly affect the critical electrical capillary number which is mostly affected by the needle diameter. Moreover, the equivalent sphere diameter is almost constant once a value twice that of the critical capillary number is exceeded. Thus, from a processing perspective there is little advantage in increasing the field strength further and this also supports the use of the smallest possible gap between the electrodes to minimise energy usage.

4.5. Upwards needle drop breakup mechanism

As stated above, when the electric potential approaches the critical values the drop size of the secondary emulsion tend to decrease in size. Regime (c_{EF}) is an innovative way to create a thin layer of water on top of oil drop which can have several applications in particular for pharmaceutical industry. This drop detachment mechanism is an alternative to the better known electro-spraying or electro-hydrodynamic modes. Thus, in the electro-spraying, the key physics involved is the reduction of interfacial tension due to electro migration in the conductive phase. This effect depends on the electric Bond number $M = \sqrt{\epsilon_0 R/2\sigma} AV_{PUL}$. The values of M of the order of magnitude of $\sim 10^{-1}$, whilst not enough to determine electro spaying, can give rise to measurable oscillations, and electrostatically-induced oscillations are reported to determine the drop breakup. However, in all the experimental cases presented in this work, M was found to be of the order of magnitude of $\sim 10^{-2}$, which suggests that electro migration is not the main contribution to the breakup. On the other hand, electro-hydrodynamic flows occur when the continuous phase has a high relative dielectric constant such as water ($\sim$80) or high electric fields are applied (10^6 V m^{-1}) in a leaky dielectric fluids. However, in this work the theory does not apply because the continuous phase has a low relative dielectric constant of 2.1 and the maximum applied voltage per unit length is $\sim 10^5$ V m^{-1}. Where electro-hydrodynamic flows could occur (primary emulsion) because the continuous phase is water, the oil drop does not change in size as shown in Fig. 5b.

The upwards detachment can be easily confused with electro dripping, but the physics involved is different. The pulling force generated by the electric field, acts on the surface drop where the negative charges are accumulated. The detachment occurs with a similar mechanism of a dripping drop (without electric field) with the difference that the mass force does not act on the drop but the electric force instead. The drop expands upwards, forming a neck at the base of the drop. The phenomenon of neck formation of thinning and pinching off is rather complex. However, it is reasonable to suppose that average flow velocity inside the neck is directed upwards towards the body of the drop. These conditions prompt the formation a negative pressure difference between the fluid inside the neck and the surrounding fluid outside it and,

consequently, the collapsing of the neck. In agreement with this, the neck was observed to collapse after ~5 ms. This caused the formation of smaller drops. Clearly, some other phenomenon contributes to this break up such as Lippmann effect which can locally decrease the tension interface of the drop, but it does not contribute as much as the electrostatic pulling force. Beside, the generated water filament does not behave as a jet which often is typical when an electric field is applied and Taylor cone is formed: no Taylor cone was observed here. Thus, the system switches from breakage to electro-coalescence which is a well-known and reported mechanism [36]. Even the dynamic interfacial tension effect is negligible in this set up because the water and surfactant solution behaves as pure liquid for a time longer than 10 ms.

Contrarily to the Regime (c_{EF}) before the critical electric potential has been reached the drop grew indefinitely at the top of the nozzle, in a position of unstable gravitational equilibrium, until it fell sideways from the nozzle under its own weight. The growth took place spherically because the sphere is the shape that allows the minimum surface for a given volume. As the energy due to the surface tension σ is proportional to the surface extension, the sphere is the shape that guarantees the minimum surface energy. This phenomenon entails an accumulation of more water into the drop which explains the larger drop than at similar fluid flow conditions with 0 kV. This phenomenon also can be confused with induced polarisation effect on the O/W interface [37], but polarisation occurs when a neutral object is immersed in an external electric field. In this work, the drop is charged by the applied high voltage through the nozzle which is a different phenomenon.

5. Conclusions

A novel technique to create O/W/O has been developed and described. This technique has great potentialities in particular for application such encapsulation and liquid coating in continuous systems, and the advantages compared with previous existing approaches have been discussed. An experimental approach to determine the effect of DC electric fields on the formation of double emulsion has been proposed in this work. Steady hydrodynamic conditions have been chosen to highlight the effect of fluid flow rate, channel diameter and electric field strength. The work shows that the electric field affects mostly the conductive phase of the emulsion (water) and that a critical AV_{PUL} (or electrical capillary number) can be identified. Below the critical value, there is little effect of the electric field and interfacial tension and gravity dominates the formation. Above the critical value, the drop size is shown to decrease rapidly and further small decreases are noted with increasing electric field strength. Various flow regimes have been identified both with and without the application of the electric field. Finally, the work shows that stable and consistent double emulsion drops can be created provided the formation of the inner oil drop is synchronised to the break-off of the water drop which contains it.

Acknowledgements

This work has been funded by the School of Chemical Engineering, University of Birmingham, UK.

We thank Dr. Emilia Nowak and Dr. Nina Kovalchuk for their help on the interfacial and surface tension measurements.

References

[1] M. Chappat, A selection of papers presented at the First World Congress on emulsions some applications of emulsions, Colloids Surf. A: Physicochem. Eng. Aspects 91 (1994) 57–77.
[2] J. Bibette, F.L. Calderon, P. Poulin, Emulsions: basic principles, Rep. Prog. Phys. 62 (6) (1999) 969.
[3] J. Yan et al., Monodisperse water-in-oil-in-water (W/O/W) double emulsion droplets as uniform compartments for high-throughput analysis via flow cytometry, Micromachines 4 (4) (2013) 402.
[4] D.A. Garrec et al., Designing colloidal structures for micro and macro nutrient content and release in foods, Faraday Discuss. 158 (2012) 37–49.
[5] N. Chiu et al., Programmed emulsions for sodium reduction in emulsion based foods, Food Function 6 (5) (2015) 1428–1434.
[6] T.K. Giri et al., Prospects of pharmaceuticals and biopharmaceuticals loaded microparticles prepared by double emulsion technique for controlled delivery, Saudi Pharm. J. 21 (2) (2013) 125–141.
[7] R. Pichot, F. Spyropoulos, I.T. Norton, O/W emulsions stabilised by both low molecular weight surfactants and colloidal particles: the effect of surfactant type and concentration, J. Colloid Interface Sci. 352 (1) (2010) 128–135.
[8] N. Garti, Double emulsions – scope, limitations and new achievements, Colloids Surf. A: Physicochem. Eng. Aspects 123 (1997) 233–246.
[9] H. Breisig et al., On the droplet formation in hollow-fiber emulsification, J. Membr. Sci. 467 (2014) 109–115.
[10] L. Hong et al., One-step formation of W/O/W multiple emulsions stabilized by single amphiphilic block copolymers, Langmuir 28 (5) (2012) 2332–2336.
[11] A.S. Utada et al., Monodisperse double emulsions generated from a microcapillary device, Science 308 (5721) (2005) 537–541.
[12] A.R. Abate, D.A. Weitz, High-order multiple emulsions formed in poly (dimethylsiloxane) microfluidics, Small 5 (18) (2009) 2030–2032.
[13] X.X. Rayleigh, On the equilibrium of liquid conducting masses charged with electricity, Philos. Mag. Ser. 5 14 (87) (1882) 184–186.
[14] J. Zeleny, Instability of electrified liquid surfaces, Phys. Rev. 10 (1) (1917) 1–6.
[15] B. Vonnegut, R.L. Neubauer, Production of monodisperse liquid particles by electrical atomization, J. Colloid Sci. 7 (6) (1952) 616–622.
[16] J.D. Sherwood, Breakup of fluid droplets in electric and magnetic fields, J. Fluid Mech. 188 (1988) 133–146.
[17] J.F. de la Mora, The fluid dynamics of Taylor cones, Annu. Rev. Fluid Mech. (2007) 217–243.
[18] E. Jens, V. Emmanuel, Physics of liquid jets, Rep. Prog. Phys. 71 (3) (2008) 036601.
[19] Á.G. Marín et al., Simple and double emulsions via coaxial jet electrosprays, Phys. Rev. Lett. 98 (1) (2007) 014502.
[20] I.I. Inculet, J.M. Floryan, R. Haywood, Dynamics of water droplets break-up in electric fields, in: Industry Applications Society Annual Meeting, 1990, Conference Record of the 1990 IEEE, 1990.
[21] J.S. Eow, M. Ghadiri, A. Sharif, Experimental studies of deformation and break-up of aqueous drops in high electric fields, Colloids Surf. A: Physicochem. Eng. Aspects 225 (1–3) (2003) 193–210.
[22] H. Kim et al., Controlled production of emulsion drops using an electric field in a flow-focusing microfluidic device, Appl. Phys. Lett. 91 (13) (2007).
[23] M. Sato, T. Hatori, M. Saito, Experimental investigation of droplet formation mechanisms by electrostatic dispersion in a liquid-liquid system, IEEE Trans. Ind. Appl. 33 (6) (1997) 1527–1534.
[24] D. Poncelet et al., Formation of microgel beads by electric dispersion of polymer solutions, AIChE J. 45 (9) (1999) 2018–2023.
[25] C.H. Yeh, M.H. Lee, Y.C. Lin, Using an electro-spraying microfluidic chip to produce uniform emulsions under a direct-current electric field, Microfluid. Nanofluid. 12 (1–4) (2012) 475–484.
[26] P.F. Salipante, P.M. Vlahovska, Electrohydrodynamics of drops in strong uniform dc electric fields, Phys. Fluids 22 (11) (2010).
[27] J.A. Lanauze, L.M. Walker, A.S. Khair, The influence of inertia and charge relaxation on electrohydrodynamic drop deformation, Phys. Fluids 25 (11) (2013).
[28] G. Taylor, Studies in electrohydrodynamics. I. The circulation produced in a drop by electrical field, Proc. Roy. Soc. Lond. A: Mathe., Phys. Eng. Sci. 291 (1425) (1966) 159–166.
[29] J.-W. Ha, S.-M. Yang, Fluid dynamics of a double emulsion droplet in an electric field, Phys. Fluids 11 (5) (1999) 1029–1041.
[30] A. Watanabe, K. Higashitsuji, K. Nishizawa, Studies on electrocapillary emulsification, J. Colloid Interface Sci. 64 (2) (1978) 278–289.
[31] Q. Xu, O.A. Basaran, Computational analysis of drop-on-demand drop formation, Phys. Fluids 19 (10) (2007).
[32] J.-W. Ha, S.-M. Yang, Fluid dynamics of a double emulsion droplet in an electric field, Phys. Fluids (1994-present), 11 (5) (1999) 1029–1041.
[33] P. Soni, V.A. Juvekar, V.M. Naik, Investigation on dynamics of double emulsion droplet in a uniform electric field, J. Electrostat. 71 (3) (2013) 471–477.
[34] Z. Bei, T.B. Jones, D.R. Harding, Electric field centering of double-emulsion droplets suspended in a density gradient, Soft Matter 6 (10) (2010) 2312–2320.
[35] A. El-Hamouz, Effect of surfactant concentration and operating temperature on the drop size distribution of silicon oil water dispersion, J. Dispersion Sci. Technol. 28 (5) (2007) 797–804.
[36] P.J. Bailes, J.G.M. Lee, A.R. Parsons, An experimental investigation into the motion of a single drop in a pulsed DC electric field, Chem. Eng. Res. Des. 78 (A3) (2000) 499–505.
[37] J.M. Santiago, D.J. Keffer, R.M. Counce, Surfactant and electric field strength effects on surface tension at liquid/liquid/solid interfaces, Langmuir 22 (12) (2006) 5358–5365.